

## Properties of Recycled and Virgin Poly(ethylene terephthalate) Blend Fibers

Joo Hyung Lee,<sup>1</sup> Ki Sub Lim,<sup>1</sup> Wan Gyu Hahm,<sup>2</sup> Seong Hun Kim<sup>1</sup>

<sup>1</sup>Department of Organic and Nano Engineering, Hanyang University, 17 Haengdang-dong, Sungdong-gu, Seoul 133-791, Korea

<sup>2</sup>Technical Textile Technology Center, Gyeonggi Technology Application Division, KITECH, Ansan 426-171, Korea

Correspondence to: S. H. Kim (E-mail: kimsh@hanyang.ac.kr)

**ABSTRACT:** Material from recycled poly(ethylene terephthalate) (PET) chips obtained from used water bottles was extruded with virgin fiber-grade PET chips in blends of 20, 40, and 70 wt %. Filament fibers from the recycled/virgin PET blends were spun using a melt spinning process and drawn by a thermal drawing process to improve their mechanical properties. As the virgin PET chips were compounded with recycled PET chips, the thermal degradation temperature ( $T_d$ ) and the melting temperature ( $T_m$ ) were increased, and the crystallization temperature ( $T_c$ ) and crystallization rate were decreased. This means that virgin PET has a better thermal stability but a lower crystallization rate than recycled PET. The double melting behavior observed in the case of the drawn fibers may have been a consequence of larger crystallites or areas of crystallites being formed during the thermal drawing process. The birefringence and mechanical properties, such as tensile strength and tensile modulus, increased and elongation at break decreased for the drawn fibers, and this was attributed to the orientation induced during crystallization. The effect of the virgin PET content in the blends on mechanical properties was investigated; 30/70 wt % recycled/virgin blended fibers showed comparable mechanical properties to virgin PET fibers. © 2012 Wiley Periodicals, Inc. *J. Appl. Polym. Sci.* 000: 000–000, 2012

**KEYWORDS:** polyesters; recycling; fibers; mechanical properties

Received 1 April 2012; accepted 11 August 2012; published online

DOI: 10.1002/app.38502

### INTRODUCTION

Resource depletion and ecological destruction are caused by the rapid growth of industry. The major problem faced by the plastics industry is waste disposal. It is necessary to promote an ecofriendly industry and to recycle waste for environmental conservation. Recently, increasing interest has been focused on the recycling of plastic waste, especially poly(ethylene terephthalate) (PET). Bottle-grade PET is one of the most commonly used packaging materials for water and beverages.<sup>1,2</sup> Unlike other polymer material waste, PET can be easily collected and recycled into useful end products.

Many researchers have investigated methods for recycling PET bottles.<sup>3,4</sup> PET recycling is one of the most successful examples of polymer recycling, and its use is widespread. The methods for recycling PET can be classified as: chemical recycling, mechanical recycling, and energy recovery (i.e., burning). The chemical recycling method involves depolymerization of the used PET to reuse the regenerated raw materials as monomers for new polymerization processes.<sup>5,6</sup> The mechanical recycling method involves re-extruding of used PET after a cleaning and shredding process.

As PET derived from used bottles has experienced heat and stress during the mechanical recycling process, the physical properties of the recycled product can be decreased. Blending of recycled PET flakes with virgin PET chips has various benefits in the industrial field, because it is a common solution used to upgrade postconsumed materials. Scaffaro and La Manta<sup>7</sup> studied blends of virgin and recycled polyamide 6 (PA 6) and found that the rheological and mechanical properties of recycled/virgin PA6 blends were improved.

According to Shen et al.,<sup>1</sup> most of the recycled PET flakes are converted into fibers. Many researchers have studied spinning recycled fibers from bottle-grade PET.<sup>8,9</sup> Abbasi et al.<sup>8</sup> have investigated the effect of the spinning speed on the physical properties of filaments from recycled bottle-grade PET.

Numerous studies have investigated the effect of the drawing process of fibers on their mechanical properties,<sup>10–14</sup> as the drawing of fibers is one of the most effective methods to improve their mechanical properties. Suzuki et al.<sup>10</sup> have studied the effect of a hot-air drawing process on PET fibers. Mahendrasingam et al.<sup>12</sup> have investigated the effect of the draw ratio and temperature on the strain-induced crystallization of PET at high draw rates.

**Table I.** Thermogravimetric Analysis of the PETR/PETV Blend Filament

Samples	$T_d^j$ (°C) <sup>a</sup>	$T_d^5$ (°C) <sup>b</sup>	Char yield (%) <sup>c</sup>
PETR/PETV (100/0 wt %)	361	390	4.4
PETR/PETV (20/80 wt %)	359	386	5.8
PETR/PETV (40/60 wt %)	375	398	7.5
PETR/PETV (70/30 wt %)	381	405	10.4
PETR/PETV (0/100 wt %)	383	402	11.3

<sup>a,b</sup>The temperature at a weight reduction of 2% and 5%, respectively.

<sup>c</sup>Residual yield in the TGA at 500°C in air.

In this research, recycled PET from waste bottles and fiber-grade virgin PET blends were prepared by melt blending process. Then, the blends were spun into filaments in an effort to improve the fiber properties of the recycle PET. Thermal drawing was performed to investigate the degree of structural development of the recycled/virgin PET blend fibers. The mechanical properties of recycled PET (PETR)/virgin PET (PETV) blend fibers were analyzed using thermogravimetric analysis (TGA), differential scanning calorimetry (DSC), birefringence measurements, and tensile tests.

## EXPERIMENTAL

### Materials

The virgin PET (PETV) chips used in this research were fiber-grade PET with an intrinsic viscosity of 0.52 dL/g, supplied by the TK Chemical Corporation (Korea). The molecular weight of the samples used was  $M_n = 18,300$  g/mol ( $M_w = 38,500$  g/mol). The recycled PET flakes (PETR) used had an intrinsic viscosity of 0.57 dL/g and were produced from a material recycling process involving used water bottles supplied by Samyang Corporation (Korea). The molecular weight of the recycled PET flake samples was  $M_n = 18,900$  g/mol ( $M_w = 43,600$  g/mol).

All the materials were dried under vacuum at 120°C for 12 h before use to eliminate any internal moisture. Then, the recycled PET flakes were compounded with virgin PET chips in several blend ratios: 20, 40, and 70 wt %, using a melt blending process in a Haake rheometer (Model 6000) equipped with a twin screw. The temperatures of heating zone, from the hopper to the die, were set to 275°C, 280°C, 280°C, and 275°C, respectively, and screw speed was fixed at 20 rpm. The recycled PET flakes and virgin PET chips were extruded under the same conditions as used for the blends to allow for a comparison.

To evaluate the effect of blending the fiber-grade virgin PET chips with the recycled PET flakes on the fiber properties, a melt spinning process was performed using PETR/PETV blends. All the samples were dried at 100°C *in vacuo* for 24 h before spinning. The blended polymer chips were melt-spun in the extruder under the following conditions: extrusion die temperature = 285°C, spinning speed = 2000 m/min, spinning nozzle = 24 holes, and nozzle diameter = 0.025 mm.

A thermal drawing process was performed to investigate the effect of drawing on the fiber properties of the recycled/virgin

PET blends. The filaments were drawn using a draw ratio of 2 at a drawing temperature of 80°C.

### Characterization

TGA (Perkin elmer Pyris 1) of the PETR/PETV blended fibers was performed under a nitrogen gas purge in the temperature range 30°C to 800°C using a heating rate of 20°C/min. The thermal behavior of the PETR/PETV blended fibers was investigated using a TA Instruments Model 2010 DSC. All the samples were heated from 30°C to 300°C using a scan rate of 10°C/min under a flowing nitrogen gas atmosphere. To eliminate any previous thermal history, the samples were held at 300°C for 5 min, and then allowed to cool to 30°C at a rate of 10°C/min. Then, the samples were heated to 300°C once again using the same heating rate as before. The thermal properties of the PETR/PETV blend fibers such as the crystallization temperature ( $T_c$ ), melting temperature ( $T_m$ ), enthalpy of crystallization ( $\Delta H_c$ ), enthalpy of melting ( $\Delta H_m$ ), and enthalpy of cold-crystallization temperature ( $\Delta T_{cc}$ ) were calculated from the DSC curves. The percentage of apparent crystallinity ( $X_c$ ) was calculated using eq. (1)<sup>15</sup>:

$$X_c(\%) = ((\Delta H_m - \Delta H_{cc})/\Delta H_m^0) \times 100 \quad (1)$$

where  $\Delta H_m^0$  is the heat of fusion of a 100% crystalline PET sample and has a value of 125.5 J/g. The birefringence of the PETR/PETV blend fibers was measured using a Nikon polarizing microscope equipped with a K-tilting compensator. The mechanical properties of the PETR/PETV blend fibers were measured at room temperature using an Instron 4454 tensile testing machine.

## RESULTS AND DISCUSSION

The TGA data of the melt spun PETR/PETV blend filament fibers with a spinning speed of 2000 m/min are summarized in Table I, and the relationship between the residual yield and the virgin PET content of the blend fibers is shown in Figure 1. The PETR as-spun filaments began to decompose at 361°C, whereas the PETV as-spun filaments were stable at higher

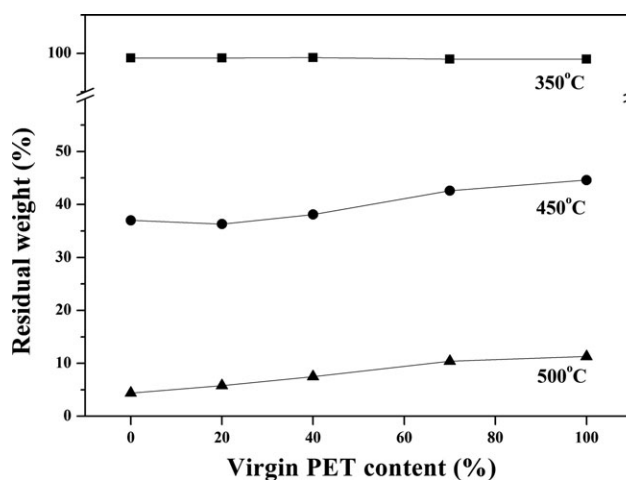


**Figure 1.** The relationship between the residual weight and virgin PET content.

**Table II.** Thermal Data for As-Spun Filaments and Drawn Fibers of PETR/PETV Blends Calculated From the DSC Curves

Sample		$T_g$ (°C)	$T_{cc}$		$T_m$		$T_{c,on}$ (°C)	$T_{c,max}$ (°C)	$T_{c,min}$ (°C)	$\Delta T_c$ (°C)
			(°C)	$\Delta H_c$ (J/g)	(°C)	$\Delta H_f$ (J/g)				
As-spun filaments	PETR/PERV(100/0)	78	127.7	-27.7	250.1	46.6	186.5	203.7	216.3	29.8
	PETR/PERV(80/20)	78	127.7	-27.4	250.7	49.8	184.2	202.6	216.0	31.8
	PETR/PERV(60/40)	78	127.9	-30.6	251.5	50.7	183.8	201.3	215.3	31.5
	PETR/PERV(30/70)	78	127.2	-28.7	251.9	48.9	179.8	200.4	216.2	36.4
	PETR/PERV(0/100)	78	127.4	-26.2	253.1	51.7	177.9	200.2	215.4	37.5
Drawn fibers	PETR/PERV(100/0)	-	94.1	-8.4	251.0	58.1	195.6	209.1	220.2	24.6
	PETR/PERV(80/20)	-	91.5	-9.2	251.6	52.1	193.7	207.6	218.7	25.0
	PETR/PERV(60/40)	-	90.5	-11.3	252.9	55.7	192.9	206.8	218.0	25.1
	PETR/PERV(30/70)	-	93.4	-6.8	253.3	53.4	187.3	205.8	217.3	30.0
	PETR/PERV(0/100)	-	91.3	-6.7	254.4	56.8	182.7	203.8	215.3	32.6

temperatures. The initial thermal degradation temperature ( $T_d^i$ ) at a 2% weight reduction and the temperature at a weight reduction of 5% ( $T_d^5$ ) in Table I revealed that the degradation temperature of the PETV filaments was higher than that of the PETR filaments by 22°C and 12°C, respectively. The thermal degradation temperature increased as the virgin PET content increased. The virgin PET content had little effect on the weight percentage of residue in the TGA at 350°C, as shown in Figure 1. However, the PETR filament fibers showed the lowest residual weight at 450°C and 500°C, respectively. The residual weight of the PETR/PETV blend filament fibers increased with increasing PETV content. Although the bottle-grade PET chips formed via a solid-state polymerization process had a higher molecular weight and higher thermal stability, they showed a lower thermal stability than that of the fiber-grade virgin PET chips used in this research that were made for automobile interiors. Therefore, by the blending of PETV to the PETR matrix, the thermal stability of the resulting PETR/PETV blend fibers can be improved.

The thermal properties, i.e., the glass transition temperature ( $T_g$ ), melting temperature ( $T_m$ ), enthalpy of melting ( $\Delta H_c$ ), and the maximum crystallization temperature ( $T_{c,max}$ ), of the as-spun filaments and drawn fibers of the PETR/PETV blends were obtained from the DSC data and are summarized in Table II. To estimate the crystallization rate in more detail, the values of the onset of and minimum crystallization temperature ( $T_{c,on}$  and  $T_{c,min}$ , respectively) and  $\Delta T_c$  ( $T_{c,on} - T_{c,min}$ ) are also summarized in Table II. The value of  $\Delta T_c$  enabled us to evaluate the change of crystallization rate. In general, when the crystallization rate increases, then the value of  $\Delta T_c$  decreases.<sup>16</sup> The cooling scans obtained from the DSC measurements of the PETR/PETV blend fibers are shown in Figure 2. In Table II and Figure 2, a broadening of the melt-crystallization peaks and a shift to lower temperatures were observed when PETV content in the PETR/PETV blends increased. This means that the PETV fibers developed a crystalline structure more slowly, and their crystallization rate was lower than that of PETR fibers. The drawn fibers had almost the same behavior as the as-spun fibers. This result is attributed to the role of the nucleants present, such as

added metal catalysts, or small molecules, such as oligomers, prepared by chain-scission reactions via thermomechanical material recycling process. An alternative explanation for this result

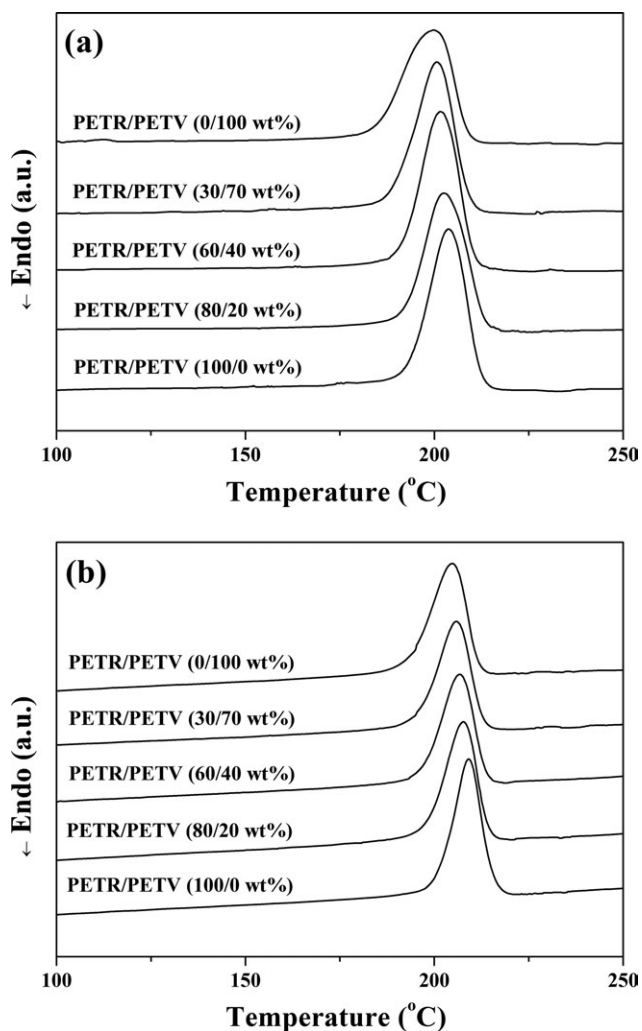


**Figure 2.** The DSC cooling scans of: (a) as-spun filaments and (b) drawn fibers of PETR/PETV blends.

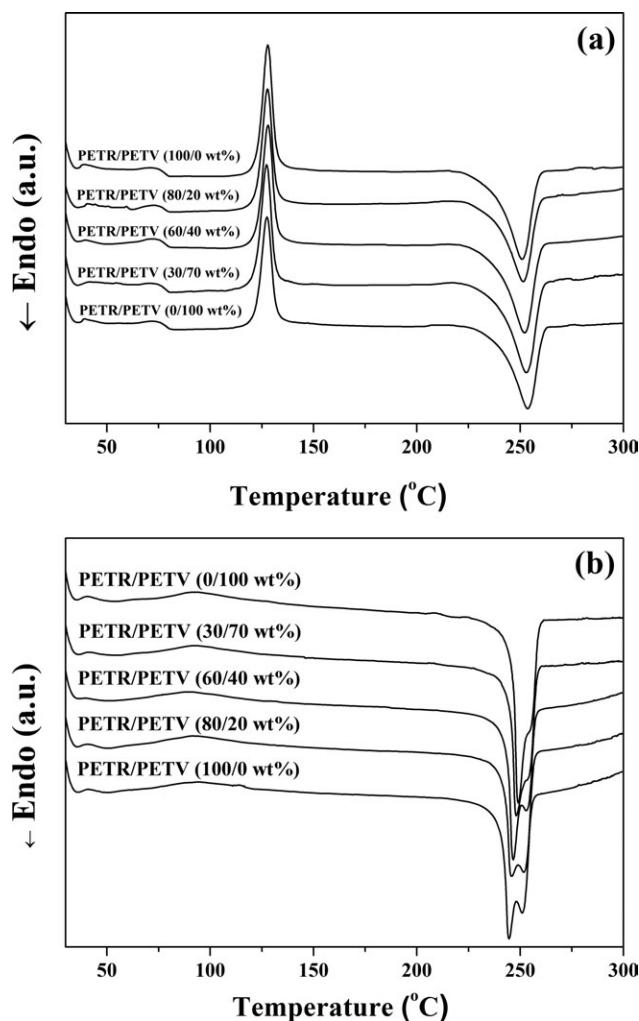


**Figure 3.** The first DSC heating scans of: (a) as-spun filaments and (b) drawn fibers of PETR/PETV blends.

is that the thermal recycling process disentangles the polymer chains, and thereby, increases the degree of crystallinity.<sup>17</sup>

Typical DSC first heating scans obtained from the PETR/PETV blend fibers are shown in Figure 3. As shown in Table II and Figure 3, the virgin PET content had little effect on the value of the glass transition temperature ( $T_g$ ). The heating scans of the as-spun filaments [Figure 3(a)] show a clear glass transition temperature ( $T_g$ ) and a cold-crystallization exotherm peak ( $T_{cc}$ ), whereas they did not show a clear  $T_g$  and  $T_{cc}$  in the case of drawn fibers [Figure 3(b)]. Compared with the as-spun filaments, the cold-crystallization exotherm peak of the drawn fibers moved to lower temperatures and decreased in magnitude. This result is attributed to development of strain-induced crystallization in the thermal drawing process. The melting temperature of the as-spun/drawn filaments of the PETR/PETV blends increased with increasing PETV content. The increase in melting temperature indicates the development of larger, more compact crystallites. The appearance of double melting peaks is shown in Figure 3(b). The change in the melting temperature ( $T_{m1}$  and  $T_{m2}$ ) is shown in Figure 4. These multiple melting

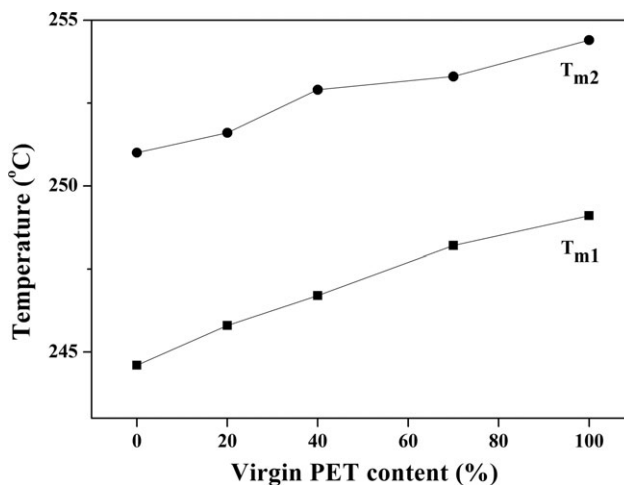


**Figure 4.** The dependence of the lower and higher melting point peaks of drawn fibers from a PETR/PERV blend on the virgin PET content.

peaks appeared regardless of the composition of the blended as-spun fibers. This indicates that this feature developed as a result of changes incurred during the postspinning process treatment. The temperatures ( $T_{m1}$  and  $T_{m2}$ ) of the multiple melting endotherms increased with increasing virgin PET content. It has been suggested that the higher temperature of the multiple melting peaks is a consequence of either the larger crystallites or areas of crystallites formed during the melt spinning or thermal drawing process. It has been suggested that the lower temperature of the double melting peak is the result of a type of structure that is formed during heat setting or the annealing process.<sup>18</sup>

The relationship between the apparent crystallinity ( $X_c$ ) calculated from the DSC data and the virgin PET content is shown in Figure 5. The degree of crystallinity of the drawn fibers increased during the drawing process, if compared with the as-spun fibers. In the case of the drawn fibers, the 80/20 wt % PETR/PETV blend fiber showed the lowest degree of crystallinity.

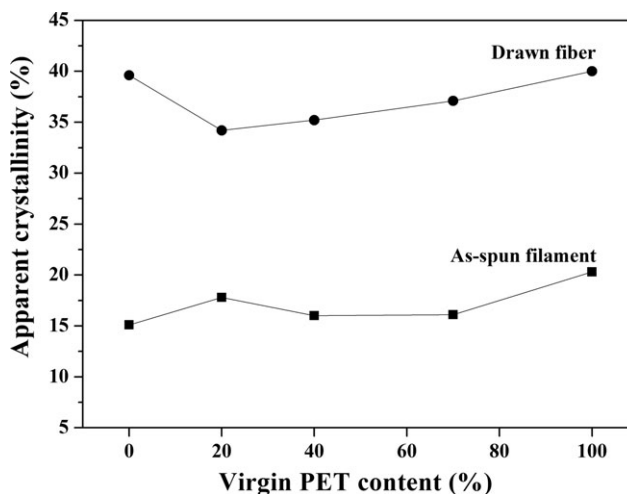


**Figure 5.** The relationship between apparent crystallinity and virgin PET content.



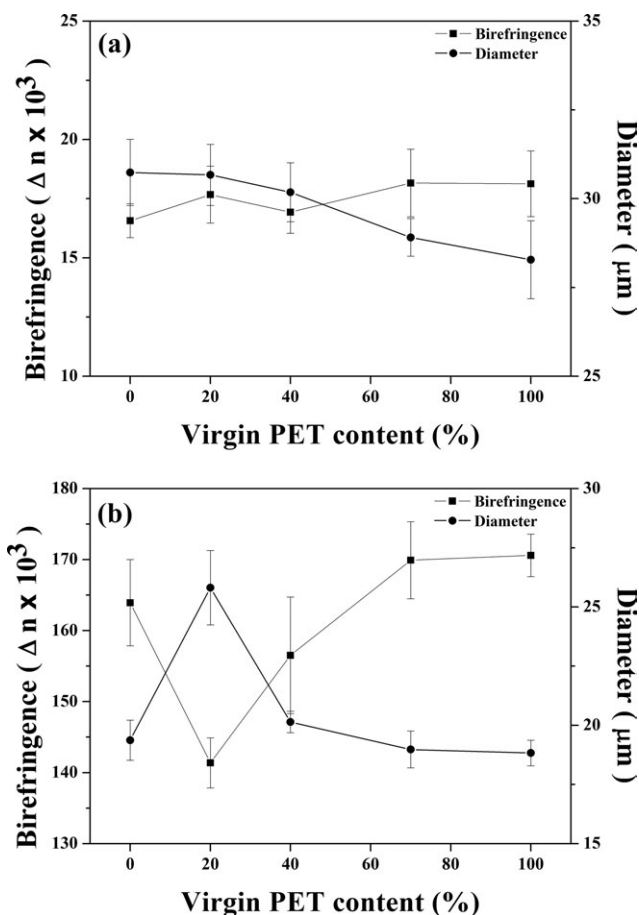


**Figure 6.** Changes in the birefringence and diameter of PETR/PETV blend fibers: (a) before and (b) after the drawing process in relation to the virgin PET content.

The dependence of the birefringence and the diameter of the PETR/PETV blend fibers on the virgin PET content before and after the drawing process are shown in Figure 6. The birefringence of the PETR/PETV blend fibers increased after the thermal drawing process, and this indicates that the orientation of the PETR/PETV blend fibers increased as the thermal drawing process was performed. Birefringence is an effective measurement of the orientation of the fibers, and so an increase in the birefringence value means that a degree of molecular orientation has developed. During the thermal drawing process, the molecular orientation of the PETR/PETV blend fibers developed, and therefore, the birefringence increased. For the as-spun filaments [Figure 6(a)], as the virgin PET content increased, the diameter of the PETR/PETV blend fibers decreased, and the birefringence value only increased slightly. The birefringence and the diameter of the PETR/PETV blend fibers represent an opposite trend, and this indicated that the higher degree of orientation of the PETR/PETV blend fibers can be attributed to the smaller diameter of the fibers. The birefringence of the PETV fibers was higher than that of the PETR fibers. Although PETV has a lower molecular weight, it can form more elongated domains orientated parallel to the fiber axis. This would result in a higher birefringence value. The birefringence of the 30/70 wt %

PETR/PETV sample showed a similar value to that of virgin PET fibers. For drawn fibers, as shown in Figure 6(b), the birefringence of the PETR/PETV blend drawn fibers with PETV contents of 70 and 100 wt % showed similar values that were higher than that of PETR drawn fibers. The birefringence of the PETR/PETV blend fibers with a PETV content of 20 and 40 wt % showed lower values than that of PETR fibers, and this was attributed to the larger diameter of the fibers. In the thermal drawing process, the 20/80 and 40/60 wt % PETR/PETV blend fibers had a less developed and ordered orientation structure. This effect decreased with increasing virgin PET content, and the 30/70 wt % PETR/PETV drawn fibers show almost the same properties as the 100 wt % PETV drawn fibers.

The dependence of the tensile strength and tensile modulus of the PETR/PETV blend fibers with the virgin PET content before and after the thermal drawing process are shown in Figure 7. The as-spun filament fibers from the 60/40 wt % PETR/PETV blend had the lowest tensile strength. The tensile strength of the 80/20 wt % PETR/PETV blend as-spun filaments was higher than that of the 60/40 wt % PETR/PETV blend fibers but lower than that of PETR fibers. The 30/70 wt % PETR/PETV blend fibers showed a higher tensile strength than PETR fibers. The PETV fibers had the highest tensile mechanical properties. As

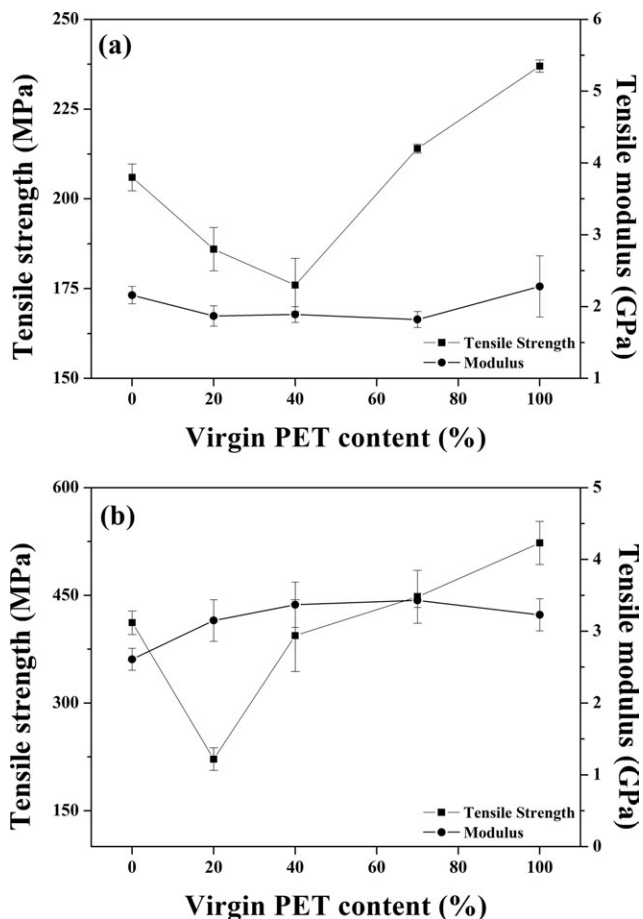


**Figure 7.** Changes in the tensile strength and tensile modulus of PETR/PETV blended fibers: (a) before and (b) after the drawing process in relation to the virgin PET content.

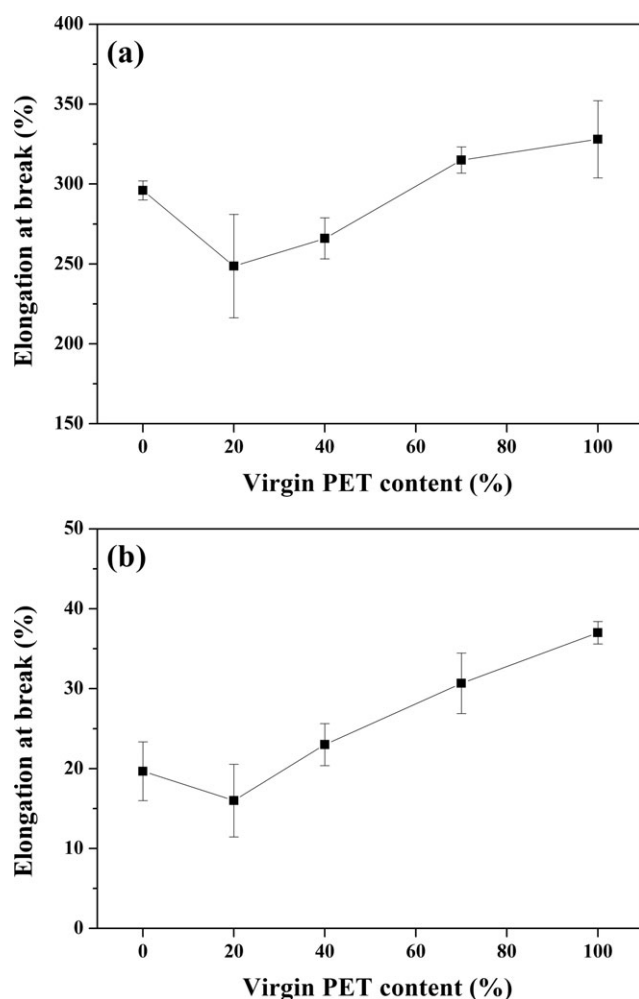


**Figure 8.** The relationship between the elongation at break and the virgin PET content of: (a) as-spun filaments and (b) drawn fibers from a PETR/PETV blend.

for the tensile modulus of the as-spun filaments, the PETV fibers showed the highest value, and the fibers from the PETR/PETV blends showed lower values than the PETR fibers. When virgin fiber-grade PET fibers were added to the recycled bottle-grade PET matrix, the mechanical properties decreased below a given critical blending proportion.

In general, the drawing process is an effective method to improve fiber properties.<sup>19</sup> Compared with as-spun filaments, the tensile strength and tensile modulus of the drawn fibers of the PETR/PETV blends increased. Drawn fibers of the 80/20 wt % PETR/PETV blend had the lowest tensile strength. This property progressively improved with increasing of virgin PET content. The PETR drawn fibers had a higher tensile strength than the 60/40 wt % PETR/PETV blend drawn fibers. The mechanical properties of the PETR/PETV blend fibers decreased on addition of a small amount of PETV to the PETR matrix. This result is attributed to the mixing of different types of PET that are made for different purposes. In the thermal drawing process, the PETR/PETV blend fibers that contained a low PETV content showed a poor structural development. However, as the

PETV content increased to about 70 wt %, the mechanical properties of the PETR/PETV blend fibers were improved.

The dependence of the elongation at break values of the PETR/PETV blend fibers on the virgin PET content before and after the thermal drawing process are shown in Figure 8. The 80/20 and 60/40 wt % PETR/PETV blend as-spun filament fibers showed lower elongation values at break point than the PETR fibers did. The 30/70 wt % PETR/PETV blend fibers showed almost equal values of elongation at break point to PETV fibers. As shown in Figure 8(b), as the virgin PET content increased, the elongation at break point increased substantially, except for the 80/20 wt % PETR/PETV blend fibers, which showed the lowest elongation at break values. This means that the PETV fibers had better properties than the PETR fibers did, and similar mechanical properties to PETV fibers could be obtained by blending a composition with about 70 wt % of PETV in the PETR matrix.

## CONCLUSIONS

PETR/PETV blend fibers with various virgin PET contents of 0, 20, 40, 70, and 100 wt % were prepared to evaluate the fiber properties of the blends, and these were subjected to a drawing process to achieve higher performance. From the TGA analysis, with increasing of the PETV content in the PETR matrix, the thermal stability was improved. From our analysis of the thermal properties using DSC, the melt-crystallization temperature and the crystallization rate decreased on mixing PETV with PETR, and this indicated that the PETR fibers exhibited a faster crystallization behavior. The melting temperature of the PETR/PETV blend fibers increased with increasing of PETV content. This result is attributed to the development of larger and more compact crystallites of PETV fibers. As a result of the thermal drawing process, drawn fibers of the PETR/PETV blends showed multiple melting endotherms and an increased degree of orientation and crystallinity, which are consistent with the increase in the birefringence values. However, blended fibers with a small amount of PETV showed a decrease in their birefringence values. Compared with the as-spun fibers, the tensile strength and tensile modulus of the drawn fibers were increased, and this was attributed to the development of a more ordered crystalline structure. Although the 80/20 and 60/40 wt % PETR/PETV blend fibers showed lower mechanical properties than the PETR fibers, the 30/70 wt % PETR/PETV blend fibers showed similar properties to PETV fibers.

## ACKNOWLEDGMENTS

This research was supported by the Ministry of Knowledge Economy of Korea; Project No. 10035180.

## REFERENCES

- Shen, L.; Worrell, E.; Patel, M. K. *Resour. Conserv. Recycl.* **2010**, *55*, 34.
- Welle, F. *Resour. Conserv. Recycl.* **2011**, *55*, 865.
- Patel, M.; Thienen, N. v.; Jochem, E.; Worrell, E. *Resour. Conserv. Recycl.* **2000**, *29*, 65.

4. Okuwaki, A. *Polym. Degrad. Stab.* **2004**, *85*, 981.
5. Shukla, S. R.; Harad, A. M.; Jawale, L. S. *Polym. Degrad. Stab.* **2009**, *94*, 604.
6. Dullius, J.; Ruecker, C.; Olivier, V.; Ligabue, R.; Einloft, S. *Prog. Org. Coat.* **2006**, *57*, 123.
7. Scaffaro, R.; La Manta, F. P. *Polym. Eng. Sci.* **2002**, *42*, 2412.
8. Abbasi, M.; Mojtahedi, M. R. M.; Khosroshahi, A. *J. Appl. Polym. Sci.* **2007**, *103*, 3972.
9. Upasani, P. S.; Jain, A. K.; Save, N.; Agarwal, U. S.; Kelkar, A. K. *J. Appl. Polym. Sci.* **2012**, *123*, 520.
10. Suzuki, A.; Nakamura, Y.; Kunugi, T. *J. Appl. Polym. Sci.* **1999**, *37*, 1703.
11. Lu, X. F.; Hay, J. N. *Polymer* **2001**, *42*, 8055.
12. Mahendrasingam, A.; Martin, C.; Fuller, W.; Blundell, D. J.; Oldman, R. J.; Harvie, J. L.; MacKerron, D. H.; Riekel, C.; Engstrom, P. *Polymer* **1999**, *40*, 5553.
13. Kim, K. H.; Yamaguchi, T.; Ohkoshi, Y.; Gotoh, Y.; Nagura, M.; Urakawa, H.; Kotera, M.; Kikutani, T. *J. Appl. Polym. Sci.* **2009**, *47*, 1653.
14. Kim, S. Y.; Kim, S. H.; Kim, J. Y.; Cho, H. H. *J. Appl. Polym. Sci.* **2007**, *104*, 205.
15. Goschel, U. *Polymer* **1996**, *37*, 4049.
16. Romão, W.; Franco, M. F.; Bueno, M. I. M. S.; De Paoli, M.-A. *Polym. Test.* **2010**, *29*, 879.
17. Fann, D.; Huang, S. K.; Lee, J. *J. Appl. Polym. Sci.* **1996**, *61*, 261.
18. Hotter, J. F.; Cuculo, J. A.; Tucker, P. A.; Annis, B. K. *J. Appl. Polym. Sci.* **1998**, *69*, 2115.
19. Mahendrasingam, A.; Martin, C.; Fuller, W.; Blundell, D. J.; Oldman, R. J.; Harvie, J. L.; MacKerron, D. H.; Riekel, C.; Engstrom, P. *Polymer* **1999**, *40*, 5553.